Talanta 220 (2020) 121439

Contents lists available at ScienceDirect

Talanta

journal homepage: www.elsevier.com/locate/talanta

Inflammatory biomarker detection in milk using label-free porous SiO_2 interferometer

D. Nanda Kumar [a,1], Nofar Pinker [b,1], Giorgi Shtenberg [a,*]

[a] Institute of Agricultural Engineering, ARO, The Volcani Center, Bet Dagan, Israel
[b] Department of Biotechnology, Faculty of Agriculture, Food and Environment, The Hebrew University of Jerusalem, Rehovot, Israel

ARTICLE INFO

Keywords:
Mastitis biomarker
NAGase
Optical biosensor
Porous silicon
Somatic cell counts

ABSTRACT

N-acetyl-β-D-glucosaminidase (NAGase) is an established indicative biomarker released upon damage or necrosis of tubular epithelial cells in both humans and animals, indicating severe nephrological disorders and bovine mastitis (BM), respectively. The latter is the most common and costly disease in dairy cattle associated with production losses, elevated somatic cell counts and deteriorated health status. Herein, we report on a reflective based assay for early diagnosis of BM through the analysis of NAGase inherent content found in whole milk samples using a miniaturized optical transducer. Gelatin functionalized porous Si Fabry–Pérot interferometers are employed for monitoring the lysosomal activity in various stages of the inflammation (healthy, subclinical and clinical). The enzymatic reaction products precipitate and accumulate within the porous nanostructure, thus alter the average refractive index monitored using reflectometric interference spectroscopy. The optical assay is calibrated within the clinically relevant concentrations of BM while presenting a dynamic range of 1.04–16.7 μM min^{-1} and the detection limit of 0.49 μM min^{-1}. The specific optical performance of the biosensor correlates with a gold standard laboratory-based approach, in which escalated somatic cell counts reveal augmented NAGase levels and thus severe pathogenesis. Overall, our study provides new opportunities to develop a convenient bio-diagnostic sensing system for BM detection and classification by addressing the limitations of conventional practices.

1. Introduction

Bovine mastitis (BM) is the most common disease of dairy cattle associated with multifactorial causes, e.g., pathogen origin, environmental contact, host-related concerns and management during the milking process, resulting in udder inflammation [1–4]. The latter is related to various causative microorganisms that include: *Staphylococcus aureus*, *Streptococci* (*uberis, dysgalactiae, agalactiae*), coliforms such as *Escherichia coli* (*E. coli*) and *Klebsiella* that can induce mammary gland pathogenesis [4,5]. BM is classified as clinical or subclinical based on the severity of the occurring disease [1,6]. The indicative symptoms in clinical BM are immediately identified as abnormal milk, udder swelling and systemic illnesses, while the subclinical statuses (>90% of all BM cases) are absent of any visible indications and thus remain undetected or untreated [3,7–9]. Conventional laboratory techniques together with cow-side rapid assays suffer from inadequacy for real-time or on-site detection of indicative BM biomarkers [4]. These biomarkers analytical performances are vastly applied for health status evaluation [10,11]. For example milk enzymes (e.g., *N*-acetyl-β-D-glucosaminidase - NAGase, alkaline phosphatase, aspartate amino transaminase, L-lactate dehydrogenase) or acute-phase proteins (e.g., milk haptoglobin, C-reactive protein, serum amyloid) have been applied for clinical and subclinical BM detection [2,4,12–14]. NAGase is an established indicative biomarker released upon damage or lysis of epithelial cells, thus indicate udder tissue impairment [8,15]. The inherent content found in milk correlates with somatic cell count (SCC) levels and can separate BM causative pathogen groups (major and minor) [16]. Overall, this intracellular lysosomal glycosidase can differentiate the entire disease spectrum (healthy, subclinical and clinical statuses) [10]. Kitchen et al. have developed a laboratory-based approach for specific NAGase activity quantification in whole milk samples [17]. Briefly, the methodology includes the specific lysosomal cleavage of 4-methylumbelliferyl-*N*-acetyl-β-D-glucosaminide (4-MUAG) substrate to a fluorogenic product of 4-methylumbelliferone (4-MU) [2,8,12,15,17]. Although

* Corresponding author.
E-mail address: giorgi@agri.gov.il (G. Shtenberg).
[1] Equal contribution.

https://doi.org/10.1016/j.talanta.2020.121439
Received 3 June 2020; Received in revised form 17 July 2020; Accepted 18 July 2020
Available online 24 July 2020

being sensitive, affordable and straightforward, the technology available more than four decades failed to implement in dairy farms [4,11].

Porous silicon (PSi) nanomaterials continue to attract immense interest for the development of effective optical sensing and biosensing platforms [18–24]. This can be attributed to the tunable features that are beneficial for biosensing transducer design, e.g., fast and simple fabrication process with controllable physical features, high surface area, tunable optical characteristics that enhance sensitivity and overall performance [25]. The optical properties of PSi thin-films are monitored using reflectometric interference spectroscopy (RIfS), which is a simple and effective method for real-time and label-free detection of any bio-interaction occurring within the porous scaffold, in correlation to refractive index changes [26]. All these features render the PSi platform as a versatile nanomaterial for biosensing applications [20,27,28].

Herein, we report on a reflective based method for BM severity diagnosis through the analysis of NAGase lysosomal activity in whole milk samples using a miniaturized optical transducer. The overall biosensing concept is illustrated in Fig. 1. PSi Fabry–Pérot interferometers are designed to detect minute biomarker content found in complex media as milk for personalized treatment decisions in dairy farms. The lysosomal activity consists of NAGase substrate-specific hydrolysis products that react with hexazonium pararosaniline reagent and precipitate instantaneously (Fig. 1a). The insoluble products infiltrate into the porous thin-film and change the reflectivity spectrum (Fig. 1b and c). The fast Fourier transform peak shift is used to link between the optical response and NAGase biochemical activity (Fig. 1d). Different milk samples at various clinical stages of BM (SCC levels and pathogen positive) are evaluated by the optical system. The transducer's performance is systematically assessed in terms of selectivity, specificity, dynamic range, limit of detection in comparison to the biochemical activity data obtained by gold standard laboratory-based approach. Our study provides new opportunities to develop a convenient bio-diagnostic sensing system for BM detection and classification by addressing the limitations of conventional practices.

2. Materials and methods

2.1. Materials

Boron-doped silicon wafers with 0.8–1.0 mΩ cm resistivity and <100> face oriented were supplied by Sil'tronix Silicon Technologies (France). Absolute ethanol (EtOH), aqueous hydrofluoric acid (HF, 48%) and analytical grade buffers were acquired from Merck Millipore (Israel). Hydrochloric acid (HCl), *N,N*-dimethylformamide (DMF), sodium hydroxide, sodium nitrite, 2-amino-2-methyl-1,3-propanediol, 3,3-dimethylglutaric acid and pararosaniline hydrochloride were supplied from Holland Moran (Israel). Acetonitrile, 3-Aminopropyltriethoxysilane (APTES), gelatin, hydrogen peroxide (H_2O_2), *N,N*-diisopropylethylamine (DIEA), *N,N′*-disuccinimidyl carbonate (DSC), NAGase suspension from bovine kidney, 4-MUAG, naphthol AS-BI *N*-acetyl-β-D-glucosaminide and naphthol AS-BI phosphate were obtained from Sigma–Aldrich Chemicals (Israel). 4-MU was supplied by Alfa Aesar (Israel).

2.2. Milk samples

The Institutional Animal Care Committee of ARO, the Volcani Center approved animal experiments (838/119IL). Milk samples were obtained from Holstein dairy cows (Volcani Center research herd) and subjected to laboratory analysis (microbiology examinations and SCC) [29]. Cows were classified upon the severity of the induced BM [11]. Briefly, milk sample with SCC <100,000 cells mL^{-1} and culture-negative were considered as healthy. Samples with SCC >200,000 cells mL^{-1}, culture-positive without visible signs, were considered as sub-clinical. Clinical BM was diagnosed by trained farm personnel at milking time, in which at least some visible signs were present (udder or milk). Those

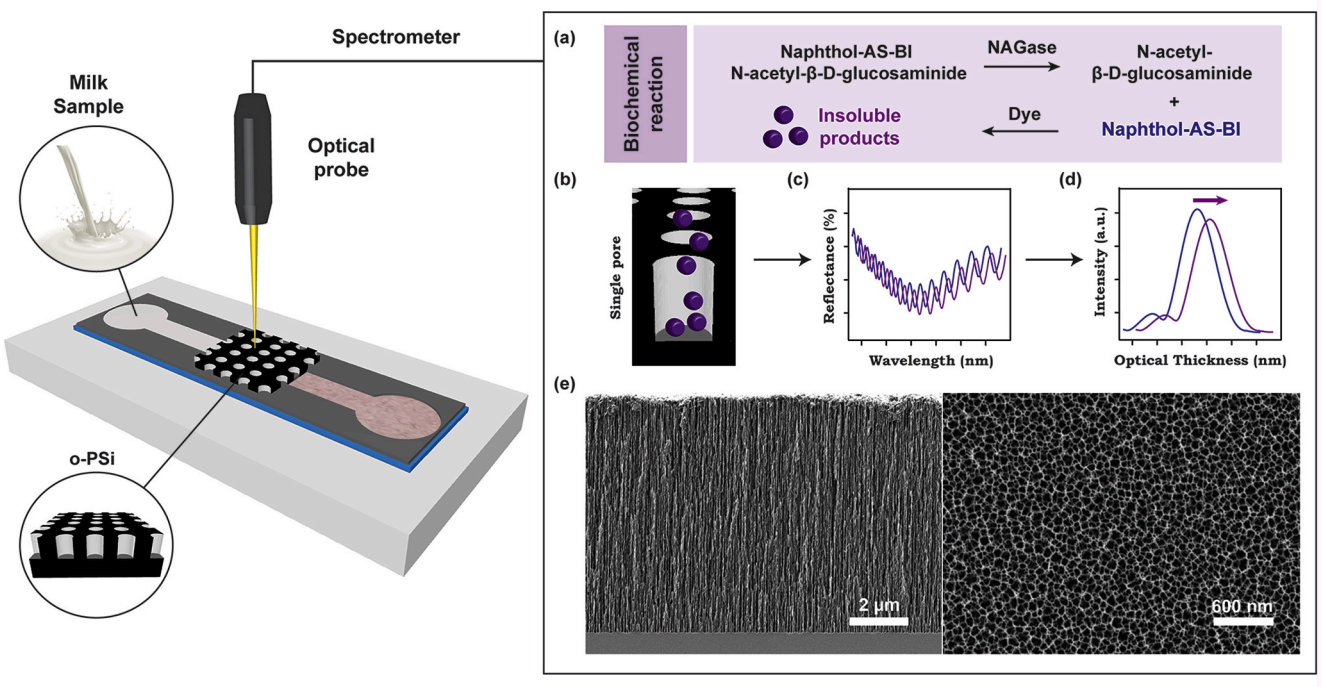

Fig. 1. Schematic representation of the optical biosensing concept for BM severity diagnosis in milk. A miniaturized optical transducer monitors the precipitation of NAGase catalytic activity products within the porous scaffold using a portable spectrometer. (a) The biochemical reaction consists of naphthol AS-BI *N*-acetyl-β-D-glucosaminide (NAGase substrate) hydrolysis into naphthol AS-BI and *N*-acetyl-β-D-glucosaminide. The addition of hexazonium pararosaniline reagent onto the solution will react with naphthol AS-BI products and will precipitate immediately; (b) The insoluble product within the pores will induce a change in (c) the reflectivity spectrum that correlates with (d) fast Fourier transform peak shift; (e) Representative HRSEM images of a typical porous scaffold (left: cross-section, right: top-view).

were later confirmed with elevated levels of SCC (>600,000 cells mL^{-1}) and positive to a pathogen.

2.3. PSi transducers preparation and modification

The PSi samples were prepared by two sequential electrochemical anodization steps of Si wafers (1.5 × 1.5 cm^2) using etching solution composed of HF (48%) and EtOH, 3 : 1 (v/v ratio), as previously described [30,31]. *Caution: HF is a highly corrosive acid - handle with extreme care.* First, a sacrificial layer was anodized at a 380 mA cm^{-2} for 30 s followed by dissolution in 0.1 M sodium hydroxide and post-polishing in 1 : 3 : 1 (v/v ratio) of HF, EtOH and ultrapure water, respectively (2 min each). Next, the second anodization of 530 mA cm^{-2} for 30 s was applied, followed by excessive EtOH wash and gentle drying under nitrogen flow. Thermal oxidation in a tube furnace (800 °C for 1 h), with a ramp rate of 20 °C min^{-1}, under ambient conditions was performed on the freshly etched PSi samples. The resulting oxidized porous platforms (o-PSi) were amino-modified by APTES and DSC cross-linker, as previously described [28]. Finally, the DSC-surfaces were reacted with 50 μL of gelatin solution (1 mg mL^{-1} in HEPES buffer, pH 7.4) for 30 min and thoroughly washed with HEPES buffer to exclude unbound proteins [27].

2.4. Milk samples pretreatment

NAGase substrate solution of 10 mM naphthol AS-BI *N*-acetyl-β-D-glucosaminide was dissolved in DMF and 3,3-dimethylglutaric acid buffer (pH 2.0) at 1 : 1 (v/v ratio). Note: milk samples were homogenizing prior to biochemical reaction. Hexazonium pararosaniline dye was prescribed by Kiernan et al. [32]. Equivalent volumes (0.5 mL) of milk and NAGase substrate solution were incubated for 1 h at 45 °C to yield *N*-acetyl-β-D-glucosaminide and naphthol AS-BI products. The latter solution was mixed with 500 μL of 2% w/v hexazonium pararosaniline reagent and 100 μL of 2-amino-2-methyl-1,3-propanediol alkaline buffer (pH 10.5), resulting in the insoluble precipitates. Control analyses in the presence of native and thermally inactivated NAGase suspensions (3.6 units each) were added to milk samples and similarly pretreated. The optical calibration curve was prepared by using known concentrations of naphthol AS-BI (62.5, 125, 250, 500 and 1000 μM) in healthy milk samples.

2.5. Reflectivity based detection of NAGase activity

A detailed description of the optical system setup and data analysis are described elsewhere [25,28,33]. The reflectance spectra were analyzed using RIfS as the effective optical thickness (EOT), proportional to the thin-film average refractive index and the total depth governed by the Fabry–Pérot equation [27,28]. In the present work, the data are presented as the relative EOT:

$$\text{Rel. EOT } (\%) = \frac{EOT_{milk\ sample} - EOT_0}{EOT_0} \times 100\% \quad (1)$$

where $EOT_{milk\ sample}$ is the optical response resulting after milk administration with respect to EOT_0 (averaged EOT values recorded during the initial optical experiment baseline). The gelatin-modified o-PSi surface was impregnated within a flow-cell and equilibrated by circulating HEPES buffer (pH 7.4) for 10 min for a stable baseline. Then, the pre-incubated milk sample mixed with the hexazonium pararosaniline reagent and the alkaline buffer was inserted and allowed to react for 1 h. Finally, the optical platform was washed with HEPES buffer (pH 7.4) to remove interfering residues. The optical experiment was completed once stable EOT values were obtained (~100 min). Surface modifications were similarly characterized by measuring the relative EOT in dry conditions, as previously noted [27].

2.6. FL based detection of NAGase activity

The enzymatic assay was performed by a modified methodology proposed by Kitchen et al. [17]. Briefly, 20 μL of milk and 80 μL of 4-MUAG (2.25 mM) in 0.25 M citrate buffer (pH 4.4) were injected into a microplate well. The biochemical reaction was reacted for 1 h at 45 °C followed by an end-point FL examination (E_m of 460 nm) [15]. The standard calibration curve was similarly prepared using fixed 4-MU concentration (0–2000 μM) in healthy milk.

2.7. Instrumentation

The morphology of o-PSi platforms was characterized by high-resolution scanning electron microscopy (HR-SEM, Carl Zeiss Ultra Plus). Surface modifications were assessed by attenuated total reflectance Fourier transform infrared (ATR-FTIR) spectroscopy using Thermo Scientific Nicolet iS50. Interferometric reflectance spectra were collected using VIS-NIR Flame spectrometer Ocean Optics (FL, USA), in a wavelength range of 500–900 nm with spectral acquisition of 80 ms saved every 30 s. The fluorescence spectra were recorded with Varioskan LUX multimode microplate reader (Thermo Scientific).

3. Results and discussion

3.1. Optical transducer design

Label-free optical biosensing platforms for the detection of NAGase activity and BM status differentiation were constructed by electrochemical anodization of heavily doped Si wafer [31]. The etching conditions were designed to entrap the biochemical reaction products within the pores by applying increased current density (530 mA cm^{-2} for 30 s). The resulting freshly prepared PSi films are then thermally oxidized to stabilize the optical platform towards aqueous media and serve as an anchoring point for surface modifications [27,34,35]. Fig. 1e depicts the structural features of the resulting nanostructure obtained by HRSEM characterization (cross-section and top-view), revealing the cylindrical-shaped pores with average size of 85 ± 10 nm and total depth of 7.8 μm. Next, the o-PSi was passivated with gelatin, a known blocking agent in immunoblot studies, to minimize the non-specific adsorption of milk constituents with the porous support [36]. The latter should hinder the fouling effect of complex media (i.e., milk samples) on the optical transducer's biosensing efficiency. Therefore, gelatin was immobilized onto the o-PSi through a standard silanization approach [28]. Fig. 2a shows the different modification steps needed to anchor gelatin onto o-PSi confirmed by RIfS studies. This technique is highly sensitive towards minute alteration in the average refractive index of the o-PSi and thus allows for direct and real-time spectral acquisition of biomolecular interactions occurring within the entire void of the porous scaffold [20,25,28,31]. The relative EOT values are proportionally increased upon bottom-up layer addition (3.0 ± 0.1, 4.3 ± 0.2, 5.1 ± 0.1% for APTES, DSC, gelatin, respectively), which correspond to the increase in the average refractive index of the porous nanostructure. Additionally, the latter immobilization step was inspected within a flow-cell configuration by injecting 50 μL of gelatin solution (1 mg mL^{-1} in HEPES buffer) onto DSC surface, Fig. 2b. Indeed, a significant increase in the relative EOT (0.70%) is shown subsequently to the gelatin solution injection that is associated with infiltration and accumulation of biomolecules within the pores. Immediately, the surface was rinsed with HEPES buffer to remove unbounded molecules from the surface resulting in a net optical response of 0.67% in the relative EOT value. ATR-FTIR spectroscopy was used as a complementary confirmation of the different surface modification, see Fig. S1 [31].

3.2. Simulated conditions for NAGase activity

The optical performance of the freshly prepared protein resistant

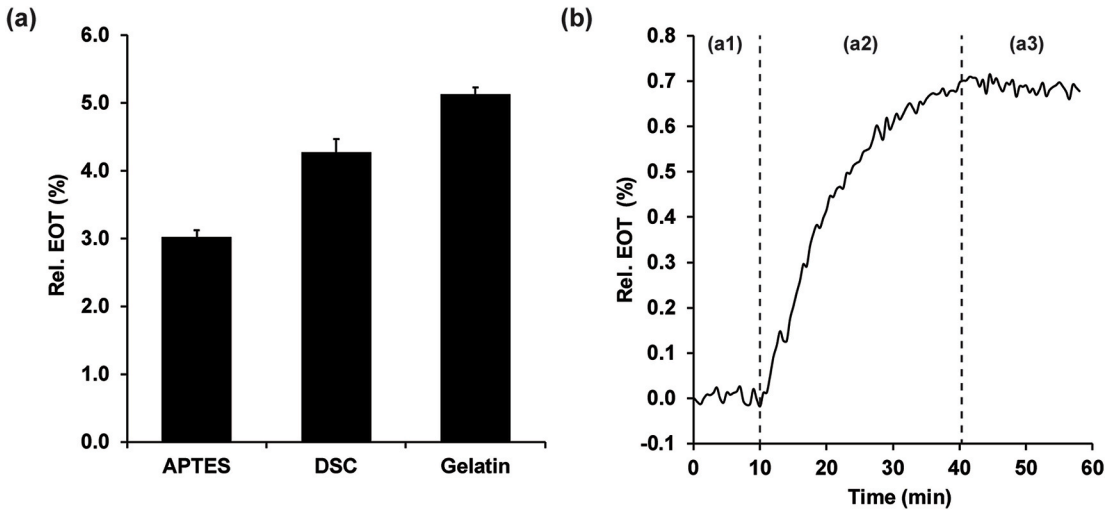

Fig. 2. Relative EOT changes following porous nanostructure modification with APTES, DSC and gelatin. The data are obtained in dry conditions and normalized with respect to the EOT value of non-modified o-PSi. Data are presented as mean ± SD ($n \geq 3$). (b) Sensorgram of DSC-modified o-PSi conjugation with gelatin. The optical transducer is pretreated with HEPES buffer to obtain a stable baseline (a1); after which gelatin solution (1 mg mL^{-1} in HEPES buffer) is introduced (a2); buffer rinsing to remove unbounded molecules (a3).

surface (gelatin-modified o-PSi) towards NAGase biochemical reaction in milk was confirmed by RIfS studies. A healthy milk sample with insignificant SCC (70,000 cells mL^{-1}) and culture-negative was set as a control sample for the assay, expecting minor NAGase activity. Fig. 3a depicts the sensorgram of gelatin-modified transducer towards the interaction with a pre-incubated milk sample mixed with hexazonium pararosaniline reagent, followed by vigorous buffer rinsing to remove any unbounded milk constituents (termed as sample milk). Indeed, a pronounced increase in the relative EOT is obtained (0.22%), suspecting the infiltration and precipitation of the reaction products, a cascade reaction of naphthol-AS-BI-*N*-acetyl-β-D-glucosaminide hydrolysis products with the dye, onto the porous thin-film. The latter optical response is associated with the biochemical reaction cascade and is verified by complementary control experiments. Native and thermally inactivated NAGase suspensions (3.6 units each) were added onto the reaction solution (containing healthy milk and NAGase substrate) while monitoring the optical response. It is expected that the addition of native NAGase suspension will induce significant optical response due to augmented biochemical reaction, producing pronounced insoluble products content within the nanostructure. In contrast, the inactivated enzyme should retain the inherent NAGase content found in a healthy milk sample, revealing minute hydrolytic activity. Fig. 3a depicts the optical output of both treatments presenting relative EOT values of 0.65 and 0.25% for native and denatured enzymes, respectively. Indeed, the latter response correlates with inherent activity found in healthy milk (without the addition of enzymatic additives), which strengthens the assumption that the EOT increase is associated with NAGase specific activity found in milk. Next, the background noise of the gelatin-modified surface was evaluated by introducing healthy milk omitting substrate from the protocol assay, followed by a vigorous rinsing process (termed as sample blank). Insignificant fouling of the nanostructure (relative EOT of 0.12%) is attained, depicting sufficient protein resistant

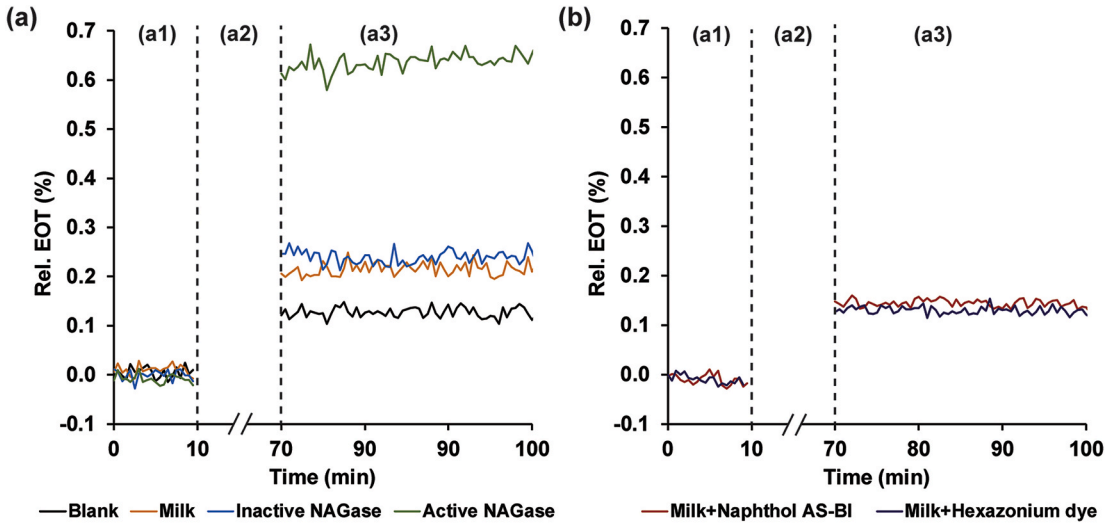

Fig. 3. Relative EOT changes vs. time of gelatin-modified o-PSi surfaces towards different milk treatments. (a) Native and thermally inactivated NAGase suspensions (3.6 units each) addition onto the reaction solution (containing healthy milk and naphthol-AS-BI *N*-acetyl-β-D-glucosaminide). Furthermore, control experiments include a healthy milk sample with and without the addition of NAGase substrate (sample milk and blank, respectively). (b) Control experiments omitting hexazonium pararosaniline reagent or naphthol-AS-BI *N*-acetyl-β-D-glucosaminide (individually) from the reaction solution. After optical baseline (a1); a mixture of the reaction solution and the dye is introduced and allowed to incubate for 1 h (a2); followed by a thorough rinsing procedure with buffer (a3).

surface, which blocks the non-specific adsorption of milk constituents. It should be highlighted that other blocking agents (e.g., skim milk, caseins, BSA, myoglobin and others) were optically analyzed, suggesting insufficient protein resistance and elevated background noise (data not shown). Finally, the selectivity of the biochemical reaction was assessed by two additional control experiments, omitting hexazonium pararosaniline reagent or NAGase substrate (individually) from the reaction solution. Fig. 3b shows the reflective based response of the assay while insignificant relative EOT values of 0.13% for both control experiments are obtained, revealing the equivalent background noise of sample blank. Overall, these results further support the attributed optical signal is ascribed to the optimal precipitation conditions of the biochemical reaction products.

3.3. Optical transducer calibration curve in milk samples

The optical calibration of the porous transducer was prepared using naphthol AS-BI (enzymatic reaction product) exposed to similar pretreatment settings. The biosensing experiments include the acquisition of stable baseline in HEPES buffer for 10 min, followed by the injection of healthy milk samples with fixed concentrations of naphthol AS-BI (62.5, 125, 250, 500 and 1000 μM) and hexazonium pararosaniline reagent. The reaction solution was allowed to incubate for 1 h and then washed vigorously to eliminate interfering residues. Fig. 4a shows the optical response of the biosensing platform towards varying naphthol AS-BI concentrations while monitoring the reflectivity spectra. The relative EOT is proportionally increased with augmented concentrations of naphthol AS-BI in the reaction solution. The resulting represent the intensified insoluble products entrapped within the o-PSi, thus increasing the averaged refractive index of the entire porous void. Fig. 4b depicts the calibration curve of the net relative EOT after subtracting sample blank values from the various naphthol AS-BI concentrations. Intensified precipitate content gradually red shifts the optical response by presenting a linear regression equation of Rel. EOT (%) = $0.0006 \times (C_{\text{naphthol AS-BI}}) - 0.0285$ ($R^2 = 0.99$). The theoretical limit of detection (LoD) of the optical system is 29.6 μM (0.49 μM min^{-1}), calculated from the regression equation as $3\sigma_a/b$, where σ_a is the standard deviation of the y-axis (floor noise) and b is the regression slope [19,37]. Moreover, the linear optical response is within the entire studied dynamic range of 62.5–1000 μM (1.04–16.7 μM min^{-1}) [2,8].

3.4. Specific NAGase activity in real milk samples

The prepared biosensing platform was applied for the detection of

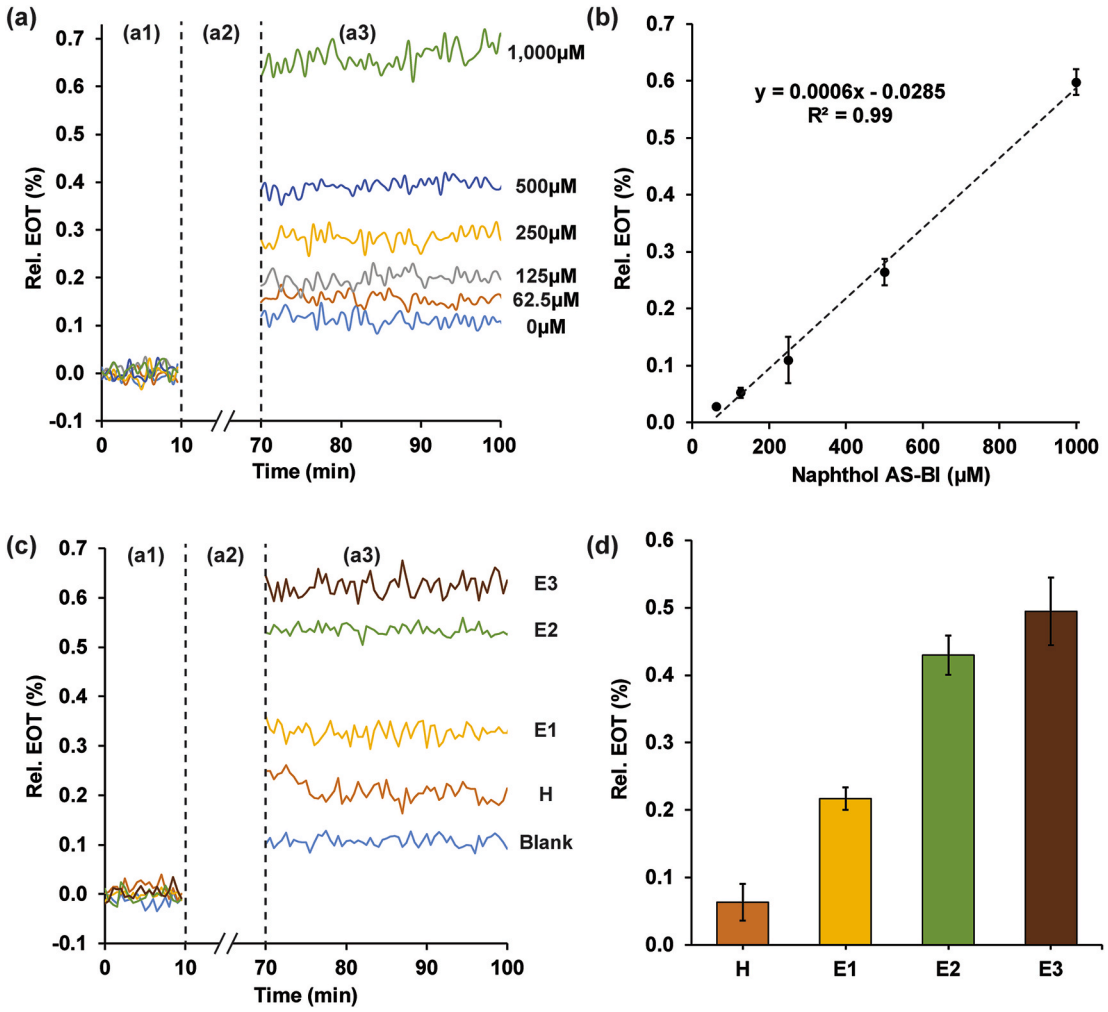

Fig. 4. Biosensing system optical calibration and real milk samples differentiation. (a) Representative relative EOT changes vs. time of the gelatin-modified o-PSi throughout the optical experiment for healthy milk samples spiked with known concentrations of naphthol AS-BI (enzymatic reaction product). (b) Calibration curve of the net optical response after subtracting sample blank relative EOT value for the different naphthol AS-BI concentrations. (c) Representative sensorgrams of NAGase catalytic activity within different milk qualities positive with *E. coli* pathogen. (d) Averaged net optical response after subtracting sample blank relative EOT value of the corresponding milk samples. Note: all sensorgrams present optical baseline acquisition (a1); a mixture of the reaction solution and the dye is introduced and allowed to incubate for 1 h (a2); followed by a thorough rinsing procedure with buffer (a3). Data are reported as mean ± SD ($n \geq 3$).

BM severity based on NAGase specific enzymatic reaction (lysosomal activity) in real milk samples. Milk samples were obtained from specific udders of Holstein dairy cows (Volcani Center research herd) within the entire disease spectrum. Table 1 summarizes the SCC and causative pathogen details of the obtained milk samples. Three SCC levels (300 and $> 600 \times 10^3$ cells mL^{-1}) for subclinical and clinical BM were studied, positive with *E. coli* (major causative pathogen) or Coagulase-negative Staphylococci (CNS, minor causative bacteria) [2–4]. Sample H (healthy milk) with insignificant SCC (70,000 cells mL^{-1}) and culture-negative was set as a control sample for the assay, expecting minor NAGase activity. It should be noted that sample H was accepted as a representative of other healthy milk samples with similar negative biological contamination and insignificant SCC values (<100,000 cells mL^{-1}). All studied samples were similarly pretreated and applied on the biosensing platform for optical inspection. Fig. 4c presents the optical sensorgrams of NAGase catalytic activity within different milk qualities positive with *E. coli*. The relative EOT values are augmented in correlation to the SCC score (0.21, 0.33, 0.53, 0.61% for H, E1, E2, E3, respectively), thus implying on the overall NAGase content. The net optical responses of the corresponding milk samples are summarized in Fig. 4d. Sample E2 and E3, both identified as clinical BM, induce significant increases in the net optical response presenting values of 0.43 ± 0.03 and 0.49 ± 0.05%, respectively. The augmented values are ascribed to the severity of the induced inflammation and pathogenesis of the analyzed animals at elevated SCC values [8]. Fig. S2 depicts similar optical response for CNS contaminated milk samples upon increased levels of SCC. It should be mentioned that the overall relative EOT values of *E.* coli contaminated samples are higher than CNS samples, as previously shown [8]. The induced inflammatory response of major pathogens results in pronounced secretion of indicative biomarkers into milk or plasma with response to minor pathogens. Finally, the net RIfS results were used to calculate NAGase specific lysosomal activity based on the fitted regression equation in comparison to conventional FL assay (Table 1). Briefly, the latter FL assay includes a non-fluorogenic substrate (4-MUAG) addition into real milk samples at various SCC levels. Inherent NAGase content will hydrolyze the 4-MUAG into a fluorescent product (4-MU) in correlation to the induced BM (Fig. S3a). The FL assay calibration curve is produced by the inclusion of known 4-MU concentrations (0–2000 μM) onto a healthy milk sample while measuring the optical output (Fig. S3b). The enzymatic activity of NAGase in different milk samples was similarly calculated and presented in Table 1. The calculated NAGase activities of both RIfS studies and the conventional FL assay in real milk samples present similar trends in which pronounced secretion of NAGase content onto milk are obtained for elevated SCC scores and at induced clinical state of the animal. Meaning, the optical results correspond with our previous reports and others, associating acute phase response with augmented enzymatic biomarker activity [2,8,10,15,38]. The RIfS recovery values are within the range of 92–109%, presenting sufficient adaptability to the conventional methodology. It should be highlighted that the sensitivity of the FL assay overpowers the reflective based approach by monitoring the emitted radiation rather than the refractive index of the porous layer, thus depicting LoD of 0.65 and 29.6 μM, respectively. Despite the lower sensitivity, the porous nanostructure assay depicts the potential to separate and to distinguish between the different clinical stages within the entire disease spectrum (i.e., healthy, subclinical and clinical) similarly to the FL assay. Overall, the developed label-free biosensing platform is sufficient for BM monitoring within real milk samples and at on-site conditions. The optical indication may serve veterinarians for early infection control and precise antimicrobial therapy, meaning only those animals requiring cure will receive it. Moreover, the use of miniaturized equipment operated at cow-side might be advantageous for new technology implementation within dairy farms. The optical platform can also be adapted for BM recovery prognosis evaluation, producing an alternative means for conventional practices.

Table 1
NAGase activity in different milk samples assessed by RIfS and by FL assay.

Sample	SCC ($\times 10^3$ cells mL^{-1})	Pathogen	RIfS (μM min^{-1})	FL assay (μM min^{-1})	Recovery (%)
H	70	N/A	1.8 ± 0.7	1.9 ± 0.3	95
E1	300	*E.coli*	6.0 ± 0.5	6.5 ± 0.1	92
E2	600	*E.coli*	11.9 ± 0.8	12.7 ± 0.2	94
E3	>1000	*E.coli*	13.7 ± 1.4	13.4 ± 0.6	102
C1	300	CNS	2.8 ± 0.8	2.6 ± 0.2	108
C2	600	CNS	4.6 ± 0.4	5.0 ± 0.3	92
C3	>1000	CNS	8.1 ± 1.2	7.4 ± 0.4	109

Data are reported as mean ± SD ($n \geq 3$).

4. Conclusions

The present work describes the application of gelatin-modified o-PSi Fabry–Pérot interferometers for monitoring NAGase activity levels in real-life conditions. Dissimilar milk samples representing all health statuses i.e., healthy, subclinical and clinical BM, were evaluated by the optical device. The obtained RIfS results correlate with gold standard FL assay, in which pronounced secretion of NAGase content onto milk were obtained for elevated SCC scores and at induced clinical state of the analyzed udders. Overall, the presented label-free optical assay can be potentially used for systematic early diagnosis of BM or for identifying new outbreaks within the herd based on indicative biomarkers found in milk. Moreover, the use of a simple and portable experimental setup could be beneficial for other analogous complex systems relevant both for human and animal diseases early detection.

Author contributions

Conceptualization, G.S.; Methodology, D.N.K., N.P. and G.S.; Validation, D.N.K. and N.P.; Formal Analysis, D.N.K., N.P. and G.S.; Investigation, D.N.K., N.P. and G.S.; Resources, G.S.; Writing—Original Draft Preparation, D.N.K. and N.P.; Writing—Review and Editing, G.S.; Visualization, D.N.K and G.S.; Supervision, G.S.; Project Administration, G.S.; Funding Acquisition, G.S.

Declaration of competing interest

The authors declare that they have no known competing financial interests or personal relationships that could have appeared to influence the work reported in this paper.

Acknowledgment

This study was supported by the JCA Charitable Foundation (459–4610).

Appendix A. Supplementary data

Supplementary data to this article can be found online at https://doi.org/10.1016/j.talanta.2020.121439.

References

[1] F. Ferrero, M. Valledor, J. Campo, Screening method for early detection of mastitis in cows, Measurement 47 (2014) 855–860.
[2] P. Kalmus, H. Simojoki, S. Pyörälä, S. Taponen, J. Holopainen, T. Orro, Milk haptoglobin, milk amyloid A, and N-acetyl-β-d-glucosaminidase activity in bovines with naturally occurring clinical mastitis diagnosed with a quantitative PCR test, J. Dairy Sci. 96 (2013) 3662–3670.
[3] P.R. Adkins, J.R. Middleton, Methods for diagnosing mastitis, Vet. Clin. 34 (2018) 479–491.
[4] C. Viguier, S. Arora, N. Gilmartin, K. Welbeck, R. O'Kennedy, Mastitis detection: current trends and future perspectives, Trends Biotechnol. 27 (2009) 486–493.
[5] G. Jones, R. Pearson, G. Clabaugh, C. Heald, Relationships between somatic cell counts and milk production, J. Dairy Sci. 67 (1984) 1823–1831.

[6] L.H. Mujawar, A. Moers, W. Norde, A. van Amerongen, Rapid mastitis detection assay on porous nitrocellulose membrane slides, Anal. Bioanal. Chem. 405 (2013) 7469–7476.
[7] N.R. Nirala, N. Pinker, C. Desitti, G. Shtenberg, Milk haptoglobin detection based on enhanced chemiluminescence of gold nanoparticles, Talanta 197 (2019) 257–263.
[8] M. Hovinen, H. Simojoki, R. Pösö, J. Suolaniemi, P. Kalmus, L. Suojala, S. Pyörälä, N-acetyl-β-D-glucosaminidase activity in cow milk as an indicator of mastitis, J. Dairy Res. 83 (2016) 219–227.
[9] C. Burvenich, V. Van Merris, J. Mehrzad, A. Diez-Fraile, L. Duchateau, Severity of E. coli mastitis is mainly determined by cow factors, Vet. Res. 34 (2003) 521–564.
[10] N.R. Nirala, G. Shtenberg, Amplified fluorescence by ZnO nanoparticles vs. Quantum dots for bovine mastitis acute phase response evaluation in milk, Nanomaterials 10 (2020) 549.
[11] S.A.M. Martins, V.C. Martins, F.A. Cardoso, J. Germano, M. Rodrigues, C. Duarte, R. Bexiga, S. Cardoso, P.P. Freitas, Biosensors for on-farm diagnosis of mastitis, Front. Bioeng. Biotech. 7 (2019).
[12] M.G. Chagunda, T. Larsen, M. Bjerring, K.L. Ingvartsen, L-lactate dehydrogenase and N-acetyl-β-D-glucosaminidase activities in bovine milk as indicators of non-specific mastitis, J. Dairy Res. 73 (2006) 431–440.
[13] M. Chagunda, N. Friggens, M.D. Rasmussen, T. Larsen, A model for detection of individual cow mastitis based on an indicator measured in milk, J. Dairy Sci. 89 (2006) 2980–2998.
[14] S. Pyörälä, M. Hovinen, H. Simojoki, J. Fitzpatrick, P. Eckersall, T. Orro, Acute phase proteins in milk in naturally acquired bovine mastitis caused by different pathogens, Vet. Rec. 168 (2011) 535.
[15] N.R. Nirala, G. Shtenberg, Enhanced fluorescence of N-acetyl-β-D-glucosaminidase activity by ZnO quantum dots for early stage mastitis evaluation, Front. Chem. 7 (2019) 754.
[16] L.M. Berning, G.E. Shook, Prediction of mastitis using milk somatic cell count, N-Acetyl-β-D-Glucosaminidase, and lactose, J. Dairy Sci. 75 (1992) 1840–1848.
[17] B. Kitchen, G. Middleton, M. Salmon, Bovine milk N-acetyl-β-D-glucosaminidase and its significance in the detection of abnormal udder secretions, J. Dairy Res. 45 (1978) 15–20.
[18] T. Tieu, M. Alba, R. Elnathan, A. Cifuentes-Rius, N.H. Voelcker, Advances in porous silicon–based nanomaterials for diagnostic and therapeutic applications, Adv. Ther. 2 (2019) 1800095.
[19] S. Mariani, A. Paghi, A.A. La Mattina, A. Debrassi, L. Dähne, G. Barillaro, Decoration of porous silicon with gold nanoparticles via layer-by-layer nanoassembly for interferometric and hybrid photonic/plasmonic (Bio)sensing, ACS Appl. Mater. Interfaces 11 (2019) 43731–43740.
[20] S. Arshavsky-Graham, N. Massad-Ivanir, E. Segal, S. Weiss, Porous silicon-based photonic biosensors: current status and emerging applications, Anal. Chem. 91 (2018) 441–467.
[21] N. Reta, A. Michelmore, C.P. Saint, B. Prieto-Simon, N.H. Voelcker, Label-free bacterial toxin detection in water supplies using porous silicon nanochannel sensors, ACS Sens. 4 (2019) 1515–1523.
[22] J. Wang, M.J. Sailor, B.-Y. Chang, Fabrication of a lateral gradient rugate in porous silicon for a miniature spectrometer application, ChemElectroChem 6 (2019) 5967–5972.
[23] X. Cheng, B. Guan, Optical biosensing and bioimaging with porous silicon and silicon quantum dots (invited review), Prog. Electromagn. Res. 160 (2017) 103–121.
[24] M. Sweetman, S. McInnes, R. Vasani, T. Guinan, A. Blencowe, N. Voelcker, Rapid, metal-free hydrosilanisation chemistry for porous silicon surface modification, Chem. Commun. 51 (2015) 10640–10643.
[25] M.J. Sailor, Porous Silicon in Practice: Preparation, Characterization and Applications, John Wiley & Sons, Weinheim, Germany, 2012.
[26] S. Kaur, C.S. Law, N.H. Williamson, I. Kempson, A. Popat, T. Kumeria, A. Santos, Environmental copper sensor based on polyethylenimine-functionalized nanoporous anodic alumina interferometers, Anal. Chem. 91 (2019) 5011–5020.
[27] G. Shtenberg, N. Massad-Ivanir, L. Fruk, E. Segal, Nanostructured porous Si optical biosensors: effect of thermal oxidation on their performance and properties, ACS Appl. Mater. Interfaces 6 (2014) 16049–16055.
[28] N. Massad-Ivanir, G. Shtenberg, A. Tzur, M.A. Krepker, E. Segal, Engineering nanostructured porous SiO2 surfaces for bacteria detection via “direct cell capture”, Anal. Chem. 83 (2011) 3282–3289.
[29] L. Martins, M.M. Barcelos, R.I. Cue, K.L. Anderson, M.V. dos Santos, J.L. Gonçalves, Chronic subclinical mastitis reduces milk and components yield at the cow level, J. Dairy Res. (2020) 1–8.
[30] G. Shtenberg, N. Massad-Ivanir, S. Engin, M. Sharon, L. Fruk, E. Segal, DNA-directed immobilization of horseradish peroxidase onto porous SiO 2 optical transducers, Nanoscale Res. Lett. 7 (2012) 443.
[31] G. Shtenberg, N. Massad-Ivanir, E. Segal, Detection of trace heavy metal ions in water by nanostructured porous Si biosensors, Analyst 140 (2015) 4507–4514.
[32] J. Kiernan, Hexazonium pararosaniline as a fixative for animal tissues, Biotech. Histochem. 79 (2004) 203–210.
[33] M.P. Schwartz, S.D. Alvarez, M.J. Sailor, Porous SiO2 interferometric biosensor for quantitative determination of protein interactions: binding of protein A to immunoglobulins derived from different species, Anal. Chem. 79 (2007) 327–334.
[34] A. Jane, R. Dronov, A. Hodges, N.H. Voelcker, Porous silicon biosensors on the advance, Trends Biotechnol. 27 (2009) 230–239.
[35] A. Janshoff, K.-P.S. Dancil, C. Steinem, D.P. Greiner, V.S.-Y. Lin, C. Gurtner, K. Motesharei, M.J. Sailor, M.R. Ghadiri, Macroporous p-Type silicon Fabry− Perot layers. Fabrication, characterization, and applications in biosensing, J. Am. Chem. Soc. 120 (1998) 12108–12116.
[36] W.Y. Craig, S.E. Poulin, M.F. Collins, T.B. Ledue, R.F. Ritchie, Background staining in immunoblot assays reduction of signal caused by cross-reactivity with blocking agents, J. Immunol. Methods 158 (1993) 67–76.
[37] R. Chhasatia, M.J. Sweetman, B. Prieto-Simon, N.H. Voelcker, Performance optimisation of porous silicon rugate filter biosensor for the detection of insulin, Sens. Actuators, B 273 (2018) 1313–1322.
[38] N.R. Nirala, Y. Harel, J.-P. Lellouche, G. Shtenberg, Ultrasensitive haptoglobin biomarker detection based on amplified chemiluminescence of magnetite nanoparticles, J. Nanobiotechnol. 18 (2020) 6.